134-W phase locking of two-dimensional four-fiber lasers with improved self-imaging resonator

Wei Wang (王 炜)[1,2], Bing He (何 兵)[1], Haibo Zhang (张海波)[1,2], Yuhao Xue (薛宇豪)[1,2], Zhen Li (李 震)[1,2], Xia Liu (刘 侠)[1,2], Jun Zhou (周 军)[1], and Qihong Lou (楼祺洪)[1*]

[1] *Shanghai Key Laboratory of All Solid-State Laser and Applied Techniques, Shanghai Institute of Optics and Fine Mechanics, Chinese Academy of Sciences, Shanghai 201800, China*

[2] *Graduate University of Chinese Academy of Sciences, Beijing 100049, China*

[*] *E-mail: qhlou@mail.shcnc.ac.cn*

Received March 3, 2010

We experimentally demonstrate the phase locking of a two-dimensional (2D) array of four fiber lasers using an improved self-imaging resonator with a spatial filter. The high visibility interference round stripes of the coherent beam profile are observed. The coherent output power of the fiber array exceeds 134 W. The entire system operates quite stably, and no thermal effects observe in the spatial filter, indicating that the coherent output power can be increased using this method.

OCIS codes: 140.3510, 140.3298.

doi: 10.3788/COL20100807.0680.

Given that the output power of one laser is limited, beam-combining technologies have been studied to solve this problem and scale the power. Coherent beam combining (CBC) and wavelength beam combining (WBC) can provide N times the power of N-element array; it can also provide N times increase in the overall radiance of the system, where the radiance is defined as the power per solid angle divided by the source aperture area[1]. In recent years, CBC has become a timely topic with the development of fiber lasers[2,3]. There are several methods that have realized CBC, such as the master oscillator power amplifier (MOPA) arrangement[4,5], self-organization mechanism in a multi-core fiber laser array[6,7], all-fiber CBC technique[8−12], self-imaging resonators, etc.[13,14]

In this letter, we experimentally demonstrate the phase locking of a two-dimensional (2D) array of four fiber lasers using a new self-imaging resonator with a spatial filter for phase locking. The pattern of the beam profile at the monitor exhibits high visibility interference round stripes. Although the individual laser optic length changes, these stripes remain in the state of relative stability. We adopt a new self-imaging resonator in order to decrease the power density on the spatial filter in the resonator. However, it has not influenced phase locking, resulting in the in-phased coherent output power of 134 W and the corresponding coherent power combination efficiency of as high as 84%. By far, this is, to our knowledge, the highest output power achieved by using the method adopted in this letter. This method is a potential approach to high power CBC.

We adopted a self-imaging cavity to create an in-phased 2D four-fiber-laser array. The experimental setup is iunstrated in Fig. 1.

Diode array lasers emitting the wavelength of 975 nm were used as pump sources. Pump beams from diode array lasers through four dichroic filters (M1) coupled into ytterbium-doped double-cladding fibers (DCFs) using four aspheric lenses (L1). The lenses used end-pumped configuration for the four fiber lasers. Four ytterbium-doped DCFs with a core diameter of 20 μm and an inner clad size of 400 μm with an octagon shape were utilized. The nominal numerical aperture (NA) was 0.06 for the core and 0.37 for the inner cladding. The lengths of the four fiber lasers were about 10, 15, 15, and 15 m, respectively. The parameters of M1 were set at a high reflectivity of more than 99.8% for 1060−1150 nm and high transmission of ∼95% for 975 nm. Four identical plano-convex lenses (L2) were placed at the output end of the fibers as the collimators. The distribution of laser array beams was 2×2. The diameters of L2 with the focal length of 18.4 mm was 6.5 mm. The distances of the centers between collimated beams were $d_x = 7.5$ mm and $d_y = 7.5$ mm. The collimated beams were placed symmetrically on the resonator optical axis on the front focal planes of the Fourier transform lens (L3) with the focal length of 500 mm. A flat mirror (M4) with more than 98% reflectivity for 1060−1150 nm was placed at the back focal panes of L3. Along the horizontal and vertical directions, we placed two platinum wires (20 μm diameter) in front of M4 to create higher loss for the out-of-phase mode. Two beam splitting prisms (M2 and M3) were placed directly on the output beam at 45°,

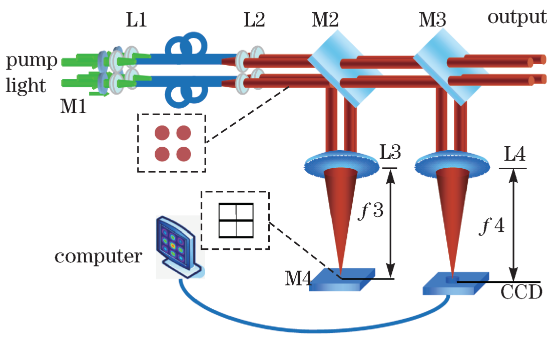

Fig. 1. Schematic diagram of experimental setup. CCD: charge-coupled device.

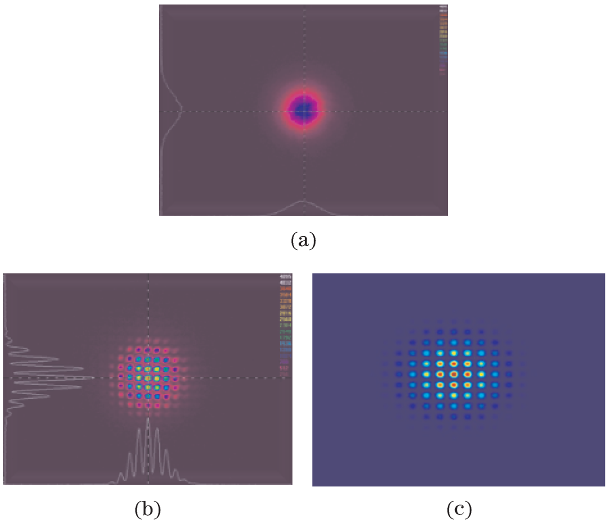

Fig. 2. Beam patterns of laser array in (a) free running, (b) in-phase, and (c) calculated in-phase modes.

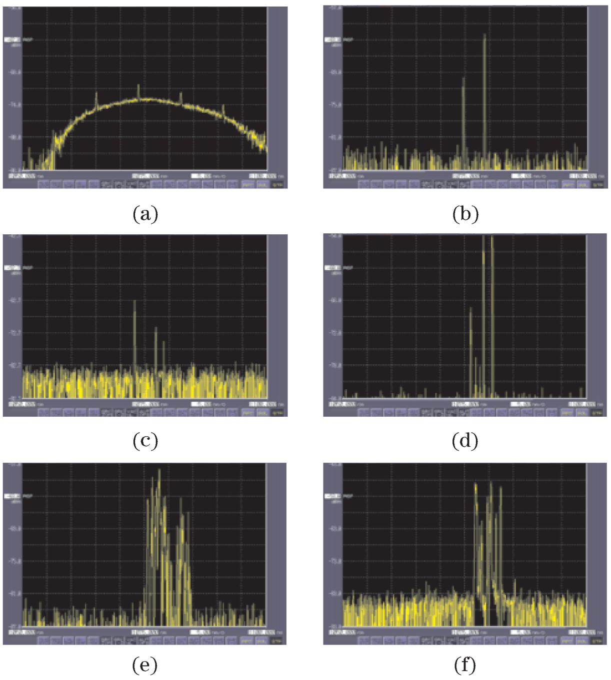

Fig. 3. Spectra of (a) F1, (b) F2, (c) F3, (d) F4 in free running, (e) combined beams without and (f) with phase-locking.

with reflectivities of 20% and 8% for 1060 and 1150 nm, respectively. We then examined the beam profile of the output beams by using a lens (L4) with the focal length of 300 mm, a CHOU4810 charge-coupled device (CCD) camera, and a laser beam analyzer (LBA-USB-SP620U; soft version 4.91; Spiricon, Inc.).

The beam profiles at the front of M2 related to each other through a Fourier transform. An arbitrary beam profile $E(x,y)$ is transformed as $E(-x,-y)$ after each round trip[15]. Thus, a symmetric beam profile around the axis of the resonator reproduces itself after every round trip, after which four beams coupled with each other. We examined the beam profile of the output at the back focal plane of L4 using a CCD camera. Figure 2(a) shows the beam profile at the back focal plane of L4 under the situation of fiber laser array, which is free-running without M4. The beam profile exhibited no interference spots. In order to stabilize the phase of the fiber laser array, M4 was placed at the back focal plane of L3. Considering high power conditions, we adopted two high melting point platinum wires with a 20-μm diameter as the spatial filter (the melting point is 1769 °C). The platinum wires were placed in a perpendicular position. Ideally, M4 should be placed at the position matching with the in-phase mode patterns, resulting in low loss for the in-phased mode and high loss for the out-of-phase mode. Figure 2(b) shows the beam profile of the in-phase mode, which exhibits high-visibility interference round spots. The calculated beam profile in the far field for the same phase between adjacent elements is shown in Fig. 2(c). The calculation was done for a separation of 7.5 mm between adjacent elements and an individual beam waist of 0.57 mm[16]. Without M4, coherent combined beam output is difficult to derive, so we obtained the coherent combined beam with M4, and the beam profile of the in-phased mode exhibited high-visibility interference round spots. The center spot width agrees well with the calculated result, the phase locking is stable even when the optical lengths are deliberately changed and mechanical perturbation is added. Given that the space duty cycle is small, the number of interference spot is large, and the power ratio of the center spot is low. In addition, once the width of the output collimated beam is allowed to increase, the power ratio of center spot will also increase.

Figures 3(a)−(d) show the different spectra of individual fiber lasers (F1−F4) in self-oscillation, respectively. Figures 3(e) and (f) show the spectra of fiber lasers in the self-imaging resonator without and with phase-locking, respectively. The fiber laser array with self-imaging resonator adhered to a self-adjusting process to adapt to optical length changes. This could be attributed to the three important properties of the fiber laser array with self-imaging resonator, namely, broad gain bandwidth, long and unequal lengths, and low-Q value. The broad gain bandwidth and long lengths provided a large number of closely spaced longitudinal modes within the gain bandwidth. The low-Q values of the resonator broadened the resonance lines to allow those near the common resonance to overlap[17]. Upon measuring the spectra of the fiber lasers with self-imaging resonator, the spaced longitudinal modes are found to be the same, whether the phase of combination beam is locked or not. Spectra

Table 1. Output Power of Combined Beams In-Phase with the Output Power of Individual Fiber Lasers

Output Power of F1 (W)	Output Power of F2 (W)	Output Power of F3 (W)	Output Power of F4 (W)	In-Phase Output Power (W)	CBC Efficiency (%)
0.65	0.65	0.55	0.55	2.29	95.4
3.27	4.36	3.05	3.05	11.78	85.8
15.81	22.25	18.97	18.97	65.43	86.1
34.90	44.06	30.97	31.30	117.77	83.4
41.77	49.95	33.70	32.82	134.13	84.8

change within a certain range of wavelength, and consequently, numerous longitudinal modes are in the output beam. In addition, the number of longitudinal modes regularly changes because of the influence of environmental variation, resulting in uncertainties in every wavelength of the longitudinal modes.

Based on the pre-experiment parameters[18], we optimize the scheme such that the output beams do not pass through M4. In this condition, the power density on M4 can be decreased without changing the output power of the beams, resulting in higher output power of the coherent beams with self-imaging resonator. As shown in Table 1, the output power of the coherent beams becomes in-phase with the output power of the fiber lasers. We obtained the 134-W output power of the coherent beams, which is by far the highest recorded value using self-imaging resonators to create CBC. The light conversion efficiency of every fiber laser is different; thus the output power of every fiber laser is different, and the highly visible interference round stripes will decrease[19].

In conclusion, we experimentally demonstrate the phase locking of a 2D array of four fiber lasers using a self-imaging resonator with a spatial filter for mode selection. The pattern of the coherent beam profile exhibits the steady interference round spots. The phase locking is due to a self-adjusting process of the fiber laser array with a long length, broad gain bandwidth, and low-Q value. The increased output power of the fiber laser array results in the 134-W output power of the in-phase coherent beam. Coherent output power can also be increased through the same method by optimizing the parameters of the resonator and the fiber laser array.

This work was supported by the Shanghai Rising-Star Program (No. 09QB1401700), the National Natural Science Foundation of China (Nos. 60908011 and 60907045), and the National "863" Program of China (No. 2008AA03Z405).

References

1. S. J. Augst, J. K. Ranka, T. Y. Fan, and A. Sanchez, J. Opt. Soc. Am. B **24,** 1707 (2007).
2. P. Zhou, Z. Liu, X. Xu, X. Wang, X. Li, and Z. Chen, Chin. Opt. Lett. **6,** 625 (2008).
3. P. Zhou, Z. Chen, X. Wang, X. Li, Z. Liu, X. Xu, J. Hou, and Z. Jiang, Chin. Opt. Lett. **6,** 523 (2008).
4. M. A. Culpepper, Proc. SPIE **4629,** 99 (2002).
5. M. Wickham, J. Anderegg, S. Brosnan, D. Hammons, H. Komine, and M. Weber, in *Advanced Solid State Photonics 2004* MA4 (2004).
6. P. K. Cheo, A. Liu, and G. G. King, IEEE Photon. Technol. Lett. **13,** 439 (2001).
7. E. J. Bochove, P. K. Cheo, and G. G. King, Opt. Lett. **28,** 1200 (2003).
8. V. A. Kozlov, J. Hernández-Cordero, and T. F. Morse, Opt. Lett. **24,** 1814 (1999).
9. T. B. Simpson, A. Gavrielides, and P. Peterson, Opt. Express **10,** 1060 (2002).
10. D. Sabourdy, V. Kermene, A. Desfarges-Berthelemot, L. Lefort, A. Barthelemy, C. Mahodaux, and D. Pureur, Electron. Lett. **38,** 692 (2002).
11. D. Sabourdy, V. Kermène, A. Desfarges-Berthelemot, L. Lefort, A. Barthélémy, P. Even, and D. Pureur, Opt. Express **11,** 87 (2003).
12. A. Shirakawa, T. Saitou, T. Sekiguchi, and K. Ueda, Opt. Express **10,** 1167 (2002).
13. C. J. Corcoran and K. A. Pasch, J. Opt. A: Pure Appl. Opt. **7,** L1 (2005).
14. C. J. Corcoran and F. Durville, Appl. Phys. Lett. **86,** 201118 (2005).
15. Y. Zhou, L. Liu, C. Etson, Y. Abranyos, A. Padilla, and Y. C. Chen, Appl. Phys. Lett. **84,** 3025 (2004).
16. C. D. Nabors, Appl. Opt. **33,** 2284 (1994).
17. L. Liu, Y. Zhou, F. Kong, Y. C. Chen, and K. K. Lee, Appl. Phys. Letts. **85,** 4837 (2004).
18. B. He, Q. Lou, W. Wang, J. Zhou, Y. Zheng, J. Dong, Y. Wei, and W. Chen, Appl. Phys. Lett. **92,** 251115 (2008).
19. W. Wang, B. He, J. Zhou, Q. Lou, X. Liu, F. Zhang, H. Zhao, and H. Xu, Acta Opt. Sin. (in Chinese) **29,** 2248 (2009).